

High pressure synthesis and characterization of the pyrochlore $\text{Dy}_2\text{Pt}_2\text{O}_7$: A new spin ice material*

Qi Cui(崔琦)^{1,2}, Yun-Qi Cai(蔡云麒)^{1,2}, Xiang Li(李翔)^{3,4}, Zhi-Ling Dun(顿志凌)^{5,6}, Pei-Jie Sun(孙培杰)^{1,2,7}, Jian-Shi Zhou(周建十)³, Hai-Dong Zhou(周海东)⁵, and Jin-Guang Cheng(程金光)^{1,2,7,†}

¹Beijing National Laboratory for Condensed Matter Physics and Institute of Physics, Chinese Academy of Sciences, Beijing 100190, China

²School of Physical Sciences, University of Chinese Academy of Sciences, Beijing 100190, China

³Materials Science and Engineering Program, Mechanical Engineering, University of Texas at Austin, Austin, Texas 78712, USA

⁴Key Laboratory of Advanced Optoelectronic Quantum Architecture and Measurement of Ministry of Education, School of Physics, Beijing Institute of Technology, Beijing 100081, China

⁵Department of Physics and Astronomy, University of Tennessee, Knoxville, TN 37996, USA

⁶School of Physics, Georgia Institute of Technology, Atlanta, GA 30332, USA

⁷Songshan Lake Materials Laboratory, Dongguan 523808, China

(Received 9 February 2020; revised manuscript received 25 February 2020; accepted manuscript online 1 March 2020)

The cubic pyrochlore $\text{Dy}_2\text{Pt}_2\text{O}_7$ was synthesized under 4 GPa and 1000 °C and its magnetic and thermodynamic properties were characterized by DC and AC magnetic susceptibility and specific heat down to 0.1 K. We found that $\text{Dy}_2\text{Pt}_2\text{O}_7$ does not form long-range magnetic order, but displays characteristics of canonical spin ice such as $\text{Dy}_2\text{Ti}_2\text{O}_7$, including (1) a large effective moment $9.64 \mu_B$ close to the theoretical value and a small positive Curie–Weiss temperature $\theta_{\text{CW}} = +0.77$ K signaling a dominant ferromagnetic interaction among the Ising spins; (2) a saturation moment $\sim 4.5 \mu_B$ being half of the total moment due to the local $\langle 111 \rangle$ Ising anisotropy; (3) thermally activated spin relaxation behaviors in the low (~ 1 K) and high (~ 20 K) temperature regions with different energy barriers and characteristic relaxation time; and most importantly, (4) the presence of a residual entropy close to Pauling’s estimation for water ice.

Keywords: $\text{Dy}_2\text{Pt}_2\text{O}_7$, pyrochlore oxide, spin ice, high-pressure synthesis

PACS: 75.10.Jm, 75.47.Lx, 75.30.-m, 75.30.Cr

DOI: 10.1088/1674-1056/ab7b58

1. Introduction

Geometrically frustrated magnets can display rich and diverse phenomena, providing an excellent platform for experimental realizations of collective magnetism that was predicted theoretically.^[1,2] The recognition of a spin ice state in the cubic pyrochlore compounds $\text{Ho}_2\text{Ti}_2\text{O}_7$ and $\text{Dy}_2\text{Ti}_2\text{O}_7$ represents such an example that successfully maps to the well-known water–ice problem.^[3–6] In these pyrochlores, the magnetic rare-earth ions, Ho^{3+} or Dy^{3+} , with a large magnetic moment of $\sim 10\mu_B$ reside on the vertices of the corner-sharing tetrahedra, forming a geometrically frustrated lattice. A uniaxial local crystalline electric field (CEF) around Ho^{3+} or Dy^{3+} results in a nearly perfect easy-axis anisotropy, forcing the rare-earth’s spin to point along the local $\langle 111 \rangle$ axis that joins the centers of two neighboring tetrahedra.^[7,8] The combination of dipolar and magnetic exchange interactions favors ‘two-in, two-out’ spin configurations on each tetrahedron, which has been termed ‘spin ice’ in direct analogy to the ‘two-short, two-long’ proton bond disorder in water ice. The Pauling’s zero-point entropy $S_P = (R/2)\ln(3/2)$, where R is the

ideal gas constant, for water ice has also been confirmed in the spin ices having a macroscopically degenerate ground state.^[5]

The low-temperature magnetic properties of a pyrochlore spin ice are mainly controlled by the magnetic exchange (J_{nn}) and the dipole–dipole interaction (D_{nn}) of the nearest-neighbor spins. For these pyrochlore spin ice materials, J_{nn} is usually antiferromagnetic, while D_{nn} is ferromagnetic and can be calculated as $D_{\text{nn}} = 5/3(\mu_0/4\pi)\mu^2/r_{\text{nn}}^3$, where r_{nn} is the nearest-neighbor rare-earth distance. D_{nn} is estimated to be ~ 2.35 K for $\text{Ho}_2\text{Ti}_2\text{O}_7$ and $\text{Dy}_2\text{Ti}_2\text{O}_7$. The physics of pyrochlore spin ices can be largely captured by the dipolar spin ice model (DSIM) proposed by den Hertog and Gingras.^[9] In the theoretical phase diagram based on DSIM,^[9] the spin ice state is stable for $J_{\text{nn}}/D_{\text{nn}} > -0.91$, and a $Q = 0$ antiferromagnetically ordered state is favored for $J_{\text{nn}}/D_{\text{nn}} < -0.91$. Since J_{nn} is more sensitive to r_{nn} than D_{nn} , by synthesizing $\text{Ho}_2\text{Ge}_2\text{O}_7$ and $\text{Dy}_2\text{Ge}_2\text{O}_7$,^[10,11] which have smaller lattice parameter in comparison to the corresponding titanates and stannates, our previous studies have successfully modified the ratio of $J_{\text{nn}}/D_{\text{nn}}$. The lowest value of -0.73 is achieved in $\text{Dy}_2\text{Ge}_2\text{O}_7$,^[11] which

*Project supported by the National Key R&D Program of China (Grant No. 2018YFA0305700), the National Natural Science Foundation of China (Grant Nos. 11834016, 11874400, and 11921004), the Beijing Natural Science Foundation, China (Grant No. Z190008), the Key Research Program of Frontier Sciences of the Chinese Academy of Sciences (Grant No. QYZDB-SSW-SLH013), and the CAS Interdisciplinary Innovation Team. ZLD and HDZ acknowledge the support of Grant No. NSF-DMR-1350002. JSZ acknowledges the support of NSF DMR Grant No. 1729588.

†Corresponding author. E-mail: jgcheng@iphy.ac.cn

is still located inside the spin ice regime. A further enhancement of J_{nn} is needed in order to achieve a transition from spin ice to a $Q = 0$ state.

Besides the chemical pressure effects caused by the size of B -cation in $Ln_2B_2O_7$ ($Ln =$ rare earth), our recent studies on the platinum-based pyrochlores $Ln_2Pt_2O_7$ have revealed an additional effect of the nonmagnetic Pt^{4+} ions,^[12,13] i.e., the spatially more extended Pt-5d orbitals and thus the enhanced Pt 5d–O 2p hybridizations can modify the CEF and influence the exchange interactions. In comparison with $Gd_2B_2O_7$ ($B =$ Ge, Ti, Sn), the antiferromagnetic transition temperature of $Gd_2Pt_2O_7$ is substantially enhanced because the empty Pt- e_g orbitals provide extra superexchange pathways.^[13] Thus, we expect an alternative routine to modify J_{nn}/D_{nn} in the Pt-based Ising pyrochlores.

In this work, we have prepared the pyrochlore compound $Dy_2Pt_2O_7$ under high pressure, and characterized its magnetic and thermodynamic properties via magnetic susceptibility and specific heat measurements down to 0.1 K. We find that $Dy_2Pt_2O_7$ does not exhibit any long-range magnetic order at low temperature, but displays canonical spin ice characteristics, including the thermally activated spin dynamics and the presence of Pauling's zero-point entropy. By comparing the low-temperature magnetic specific heat to DSIM, we obtain a ratio of $J_{nn}/D_{nn} = -0.56$ for $Dy_2Pt_2O_7$. Our results demonstrate that $Dy_2Pt_2O_7$ is a new spin ice compound with enhanced superexchange interaction J_{nn} .

2. Experimental details

The sample preparations and characterizations in the present study are similar to those performed in our previous work.^[12] The cubic pyrochlore $Dy_2Pt_2O_7$ sample was prepared under 4 GPa and 1000 °C by using a Kawai-type multi-anvil module (Max Voggenreiter GmbH). The resultant high-pressure products were first washed with warm aqua regia to remove a small amount of platinum metal and unreacted Dy_2O_3 ; the obtained powders were then pressed into pellets and subjected to heat treatment at 900 °C for 10 h to facilitate the measurements of the bulk physical properties.

Phase purity of the obtained powder and pellet samples was examined by powder x-ray diffraction (XRD) at room temperature. Structural parameters were extracted from the XRD patterns via Rietveld refinement with the FullProf program. DC magnetic susceptibility was measured with a commercial magnetic property measurements system (MPMS-III, Quantum Design) in the temperature range from 1.8 K to 300 K under an external magnetic field of $\mu_0 H = 0.1$ T. AC magnetic susceptibility measurements in the temperature range $2 \text{ K} < T < 50$ K were performed in a physical property measurement system (PPMS, Quantum Design). AC susceptibility measurements from 70 mK to 2 K were carried out in an

Oxford dilution refrigerator with the mutual induction method; an excitation current of ~ 1 mA with frequencies ranging from 117 Hz to 1517 Hz was applied to the primary coil during the measurements. Specific-heat data down to 0.1 K were collected by the PPMS with a dilution refrigerator insert.

3. Results and discussion

3.1. Structure characterizations

Figure 1 (a) shows the powder XRD pattern of $Dy_2Pt_2O_7$, which is confirmed to be single phase with the pyrochlore structure. The XRD pattern can be refined well with a cubic pyrochlore structure defined by the $Fd-3m$ (No. 227) space group with the Dy atom at $16d$ ($1/2, 1/2, 1/2$), the Pt atom at $16c$ ($0, 0, 0$), the O1 atom at $48f$ ($x, 1/8, 1/8$), and the O2 atom at $8b$ ($3/8, 3/8, 3/8$) site, respectively. The obtained lattice constant $a = 10.1913(1)$ Å for $Dy_2Pt_2O_7$ is in excellent agreement with the previously reported value of 10.202 Å.^[14] In addition, the lattice constant a scales linearly with the ionic radius (IR) of the B^{4+} ions for the series of $Dy_2B_2O_7$ ($B =$ Sn, Pt, Ti, Ge), as depicted in Fig. 1(b).

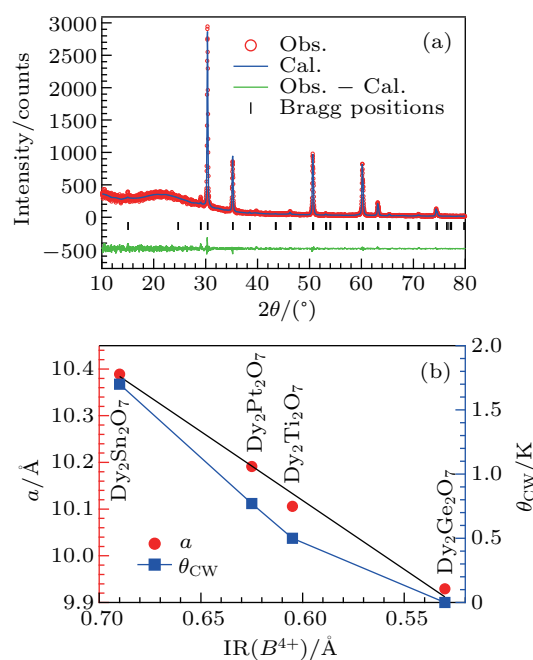


Fig. 1. (a) Room-temperature powder XRD pattern of $Dy_2Pt_2O_7$ and the results of the Rietveld refinement. (b) Lattice parameter a (left) and the Curie–Weiss temperature θ_{CW} (right) as a function of the ionic radius of the B^{4+} ions in the series of $Dy_2B_2O_7$ ($B =$ Sn, Pt, Ti, Ge).

3.2. DC magnetic susceptibility

The magnetic properties of $Dy_2Pt_2O_7$ were first characterized by DC magnetization measurements in the temperature range from 1.8 K to 300 K. Figure 2(a) displays the DC magnetic susceptibility $\chi(T)$ and its inverse $\chi^{-1}(T)$ measured under $\mu_0 H = 0.1$ T after zero-field-cooled (ZFC) and field-cooled (FC) processes from room temperature. No sign of long-range magnetic ordering was observed down to 1.8 K.

A Curie–Weiss (CW) fitting has been applied to $\chi^{-1}(T)$ in the temperature range 10–50 K, i.e., $\chi^{-1}(T) = (T - \theta_{\text{CW}})/C$, which yields an effective moment $\mu_{\text{eff}} = 9.62 \mu_{\text{B}}$ per Dy^{3+} and a CW temperature $\theta_{\text{CW}} = +0.77 \text{ K}$ for $\text{Dy}_2\text{Pt}_2\text{O}_7$. The obtained μ_{eff} is very close to the theoretical value of $9.55 \mu_{\text{B}}$ for free Dy^{3+} ion with $J = 15/2$, and the small positive θ_{CW} signals a net ferromagnetic interaction between the Ising spins located on the vertices of the corner-shared tetrahedra.^[15] As seen in Fig. 1(b), the positive θ_{CW} decreases roughly linearly with decreasing IR of B^{4+} and approaches to zero for the Ge-based pyrochlore. Such a monotonic variation of θ_{CW} versus IR(B^{4+}) suggests that the nearest-neighbor distance, r_{nn} , remains the dominant factor that governs the balance between the antiferromagnetic J_{nn} and the ferromagnetic D_{nn} between the nearest-neighbor Ising spins.

The isothermal magnetization $M(H)$ curves measured in fields up to 5 T at 2 K and 5 K are shown in Fig. 2(b) for $\text{Dy}_2\text{Pt}_2\text{O}_7$. As seen in the classical spin ices, a typical ferromagnetic behavior is observed and the saturation moment reaches $\sim 4.5 \mu_{\text{B}}$ per Dy^{3+} , which is about half of the total moment available at each site due to the local $\langle 111 \rangle$ Ising magnetic anisotropy and the powder averaging.^[16] From these DC magnetic measurements on $\text{Dy}_2\text{Pt}_2\text{O}_7$, we find nearly identical behaviors as those well-characterized classical spin ices $\text{Dy}_2\text{B}_2\text{O}_7$ ($B = \text{Sn, Ti, Ge}$). Below we further provide the AC magnetic susceptibility and thermodynamics evidences in support of the spin-ice behavior for $\text{Dy}_2\text{Pt}_2\text{O}_7$.

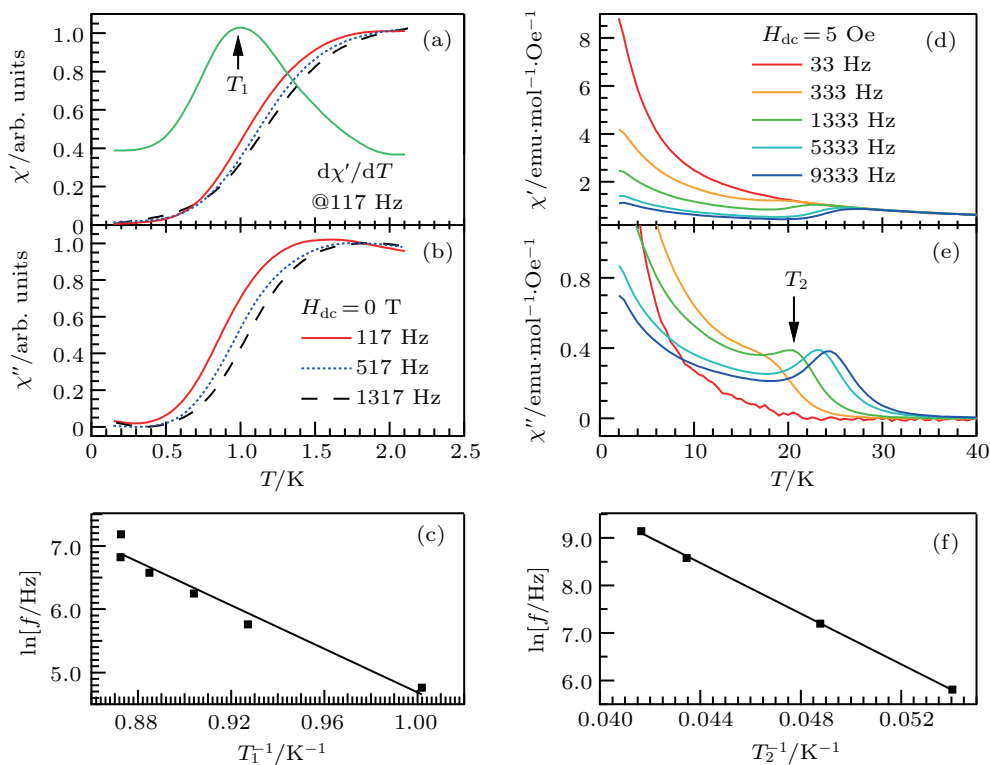


Fig. 3. The real part $\chi'(T)$ and the imaginary part $\chi''(T)$ of the AC magnetic susceptibility for $\text{Dy}_2\text{Pt}_2\text{O}_7$ in the temperature range (a), (b) below 2 K and (d), (e) above 2 K. (c) and (f) The linear fit to the Arrhenius plot of the characteristic temperatures T_1 and T_2 , respectively.

3.3. AC magnetic susceptibility

Figure 3 shows the AC magnetic susceptibility of $\text{Dy}_2\text{Pt}_2\text{O}_7$ in the temperature range (a)–(c) below 2 K and (d)–(f) above 2 K. For $T < 2 \text{ K}$, the real $\chi'(T)$ and the imaginary part $\chi''(T)$ are normalized by their maximum values.

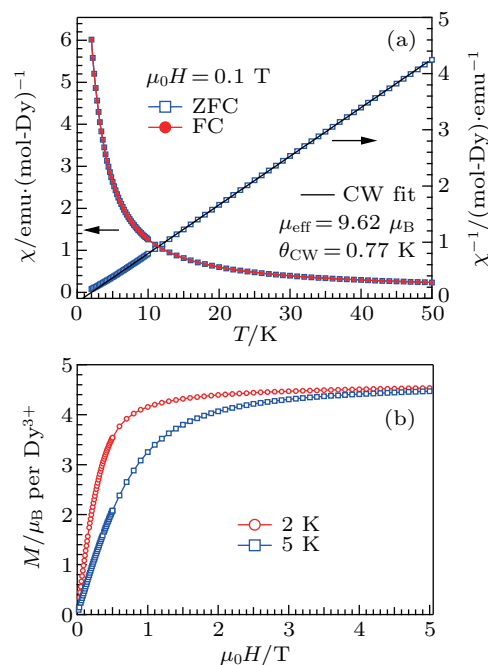


Fig. 2. (a) Temperature dependence of the DC magnetic susceptibility $\chi(T)$ and its inverse $\chi^{-1}(T)$ for $\text{Dy}_2\text{Pt}_2\text{O}_7$. The solid line represents the Curie–Weiss fitting curve and the fitting parameters are given in the figure. (b) The isothermal magnetization curves $M(H)$ measured at $T = 2 \text{ K}$ and 5 K for $\text{Dy}_2\text{Pt}_2\text{O}_7$.

As can be seen in Figs. 3(a) and 3(b), $\chi'(T)$ in the frequency range from 117 Hz to 1317 Hz drops quickly below ~ 1.6 K, and $\chi''(T)$ displays a broad shoulder at a slightly lower temperature. Both $\chi'(T)$ and $\chi''(T)$ are frequency dependent and the shoulder shifts to higher temperatures upon increasing frequency. Such a slow spin dynamics is typical for classical spin ices and has been attributed to the formation of spin-ice configurations.^[17,18] Due to the ambiguity of the maximum in $\chi''(T)$, here we define the maximum of $d\chi'/dT$ as a characteristic temperature T_1 whose frequency dependence can be fitted with an Arrhenius formula, $f = f_{01} \exp(-E_{a1}/\kappa_B T_1)$, Fig. 3(c), yielding an activation energy $E_{a1}^{\text{Dy}} = 17.2(1.8)$ K and a characteristic relaxation time $\tau_{01}^{\text{Dy}} = 1/f_{01}^{\text{Dy}} = 3.18 \times 10^{-10}$ s.

Another distinct feature in the AC susceptibility of Dy-pyrochlore spin ices is the presence of a high-temperature peak around 15 K.^[17–20] Similar behaviors are also observed in $\text{Dy}_2\text{Pt}_2\text{O}_7$, Figs. 3(d) and 3(e). For $f \geq 333$ Hz, we observe a clear drop in $\chi'(T)$ and a corresponding maximum in $\chi''(T)$ at temperature T_2 , which starts at ~ 18 K and moves to higher temperatures with increasing frequency. Similarly, a linear fitting to the Arrhenius plot of $\ln f$ versus $1/T_2$, Fig. 3(f), gives the activation energy $E_{a2}^{\text{Dy}} = 267(4)$ K and the characteristic relaxation time $\tau_{02}^{\text{Dy}} = 1/f_{02}^{\text{Dy}} = 1.66 \times 10^{-9}$ s, which are also consistent with the reported values of $E_a = 210$ K and $\tau_0 = 1.39 \times 10^{-9}$ s for the polycrystalline $\text{Dy}_2\text{Ti}_2\text{O}_7$.^[20] Since the energy barrier $E_{a2} \sim 300$ K is close to the energy scale set by the first excited CEF level from the ground state doublet, the spin relaxation processes are thermally activated for $T \geq T_2$.

3.4. Specific heat

Figure 4(a) shows the low-temperature specific heat $C(T)$ of $\text{Dy}_2\text{Pt}_2\text{O}_7$, which displays a Schottky-like peak centered at about 1.1 K. Both the peak position ~ 1 K and the magnitude $\sim 3 \text{ J}\cdot(\text{mol}\cdot\text{Dy})^{-1}\cdot\text{K}^{-1}$ are very similar to those of the classical Dy-pyrochlore spin ices, $\text{Dy}_2\text{B}_2\text{O}_7$ ($B = \text{Sn}, \text{Ti}, \text{Ge}$).^[11] The magnetic contribution C_m was obtained by subtracting from the measured total specific heat C_{total} the lattice contribution C_{lat} , which was taken from the specific heat of isostructural, nonmagnetic $\text{Lu}_2\text{Pt}_2\text{O}_7$. As shown in Fig. 4(a), the magnetic entropy obtained via integrating C_m/T over the investigated temperature range approaches a constant value of $\sim 4.2 \text{ J}\cdot(\text{mol}\cdot\text{Dy})^{-1}\cdot\text{K}^{-1}$, which falls considerably short of the expected value of $R\ln 2 \approx 5.76 \text{ J}\cdot(\text{mol}\cdot\text{Dy})^{-1}\cdot\text{K}^{-1}$ for Dy^{3+} with a ground Karmers doublet. The resultant residual entropy $1.56 \text{ J}\cdot(\text{mol}\cdot\text{Dy})^{-1}\cdot\text{K}^{-1}$ is close to the Pauling's zero-point entropy $S_P = (R/2)\ln(3/2) = 1.68 \text{ J}\cdot(\text{mol}\cdot\text{Dy})^{-1}\cdot\text{K}^{-1}$, providing an important evidence for the spin-ice state in $\text{Dy}_2\text{Pt}_2\text{O}_7$.^[5]

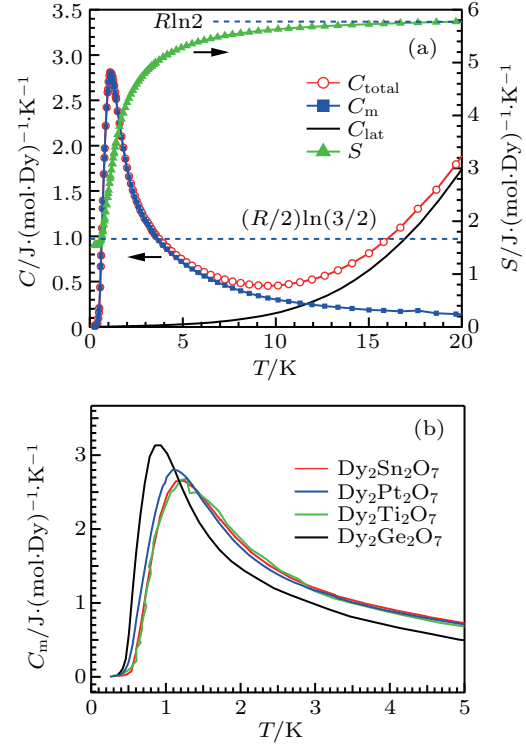


Fig. 4. (a) Specific heat $C(T)$ of $\text{Dy}_2\text{Pt}_2\text{O}_7$. The $C(T)$ of isostructural, nonmagnetic $\text{Lu}_2\text{Pt}_2\text{O}_7$ was used as the lattice contribution C_{lat} . The magnetic contribution C_m was obtained by subtracting C_{lat} from the measured total C_{total} . The entropy S was evaluated by integrating C_m/T over the investigated temperature range. (b) Comparison of the magnetic specific heat C_m of $\text{Dy}_2\text{B}_2\text{O}_7$ ($B = \text{Sn}, \text{Pt}, \text{Ti}, \text{Ge}$) pyrochlores.

3.5. Discussion

Based on these above characterizations, we can conclude that $\text{Dy}_2\text{Pt}_2\text{O}_7$ is a new spin ice characterized by: (i) a large effective moment $9.64 \mu_B$ close to the theoretical value, and a small positive Curie–Weiss temperature $\theta_{\text{CW}} = +0.77$ K signaling a dominant ferromagnetic interaction among the Ising spins; (ii) a saturation moment $\sim 4.5 \mu_B$ being half of the total moment due to the local $\langle 111 \rangle$ Ising anisotropy; (iii) thermally activated spin relaxation behaviors in the low (~ 1 K) and high (~ 20 K) temperature regions with different energy barriers and characteristic relaxation time; and most importantly, (iv) the presence of a residual entropy close to Pauling's estimation for water ice.

Although it is not unexpected that $\text{Dy}_2\text{Pt}_2\text{O}_7$ displays typical behaviors of canonical spin ice, the effects of nonmagnetic Pt^{4+} are noteworthy. For this purpose, we have compared the C_m of $\text{Dy}_2\text{Pt}_2\text{O}_7$ with those of $\text{Dy}_2\text{B}_2\text{O}_7$ ($B = \text{Sn}, \text{Ti}, \text{Ge}$) in Fig. 4(b). For those latter spin ices, it has been shown that the C_m peak shifts to lower temperatures and its height also increases upon reducing the ionic radius of B^{4+} ions or r_{nn} .^[11] This is consistent with the prediction of DSIM due to the enhancement of J_{nn} with respect to D_{nn} .^[9] If considering only the lattice parameter or r_{nn} , the C_m peak of $\text{Dy}_2\text{Pt}_2\text{O}_7$ should locate in between those of $\text{Dy}_2\text{Sn}_2\text{O}_7$ and $\text{Dy}_2\text{Ti}_2\text{O}_7$. However, as shown in Fig. 4(b), the C_m peak of $\text{Dy}_2\text{Pt}_2\text{O}_7$ is higher than that of $\text{Dy}_2\text{Sn}_2\text{O}_7$ and $\text{Dy}_2\text{Ti}_2\text{O}_7$, and the C_m

peak also occurs at a lower temperature than the other two. Based on the prediction of DSIM^[9] and $D_{nn} \approx 2.29$ K for Dy₂Pt₂O₇, the C_m peak temperature $T_{\text{peak}} = 1.13$ K corresponds to a $J_{nn}/D_{nn} = -0.56$, which predicts $J_{nn} = -1.28$ K and $J_{\text{eff}} = J_{nn} + D_{nn} = 1.01$ K. These values are also listed in Table 1. For comparison, Dy₂Ti₂O₇ has $J_{nn}/D_{nn} = -0.49$, $J_{nn} = -1.15$ K, and $J_{\text{eff}} = 1.20$ K.^[11] Because the ionic radius of Pt⁴⁺ (0.625 Å) is larger than that of Ti⁴⁺ (0.605 Å), the observed larger $|J_{nn}|$ and $|J_{nn}/D_{nn}|$ in Dy₂Pt₂O₇ than those of Dy₂Ti₂O₇ suggest that other factors beyond the chemical pressure effect should play a role in determining the low-temperature magnetic properties of Dy₂Pt₂O₇. As in the case of Gd₂Pt₂O₇,^[13] we attribute the enhanced $|J_{nn}|$ in Dy₂Pt₂O₇ to the extra superexchange pathways through the empty e_g orbitals of Pt⁴⁺ via Dy–O–Pt–O–Dy. This contribution becomes prominent in Dy₂Pt₂O₇ having the spatially more extended Pt 5d orbitals.

Table 1. Lattice parameter and selected magnetic parameters for the Dy-pyrochlore spin ices Dy₂B₂O₇ (B = Ge, Ti, Pt, Sn).

Dy ₂ B ₂ O ₇	Ge	Ti	Pt	Sn
IR(B^{4+})/Å	0.53	0.605	0.625	0.69
$a/\text{Å}$	9.93	10.10	10.1913(1)	10.40
$\theta_{\text{CW}}/\text{K}$	0	0.5	0.77	1.7
D_{nn}/K	2.47	2.35	2.29	2.15
$C_{\text{peak}}/J \cdot (\text{mol-Dy})^{-1} \cdot \text{K}^{-1}$	3.17	2.72	2.80	2.65
T_{peak}/K	0.828	1.25	1.13	1.20
J_{nn}/D_{nn}	-0.73	-0.49	-0.56	-0.46
J_{eff}/K	0.67	1.2	1.01	1.16
Ref.	[11]	[11]	this work	[11]

4. Conclusion

In summary, we have synthesized the cubic pyrochlore Dy₂Pt₂O₇ under 4 GPa and 1000 °C, and confirmed it to be a new classical spin ice as Dy₂Ti₂O₇. The magnetic specific heat of Dy₂Pt₂O₇ signals a moderate enhancement of $|J_{nn}|$, but the ratio $J_{nn}/D_{nn} = -0.56$ remains located in the spin ice regime as predicted by DSIM. Our work demonstrates that the

J_{nn}/D_{nn} can be effectively tuned by replacing the B-site cation of Ising pyrochlores. But further explorations are needed to realize a transition from spin ice to an antiferromagnetically ordered state by varying J_{nn}/D_{nn} in a larger range as predicted by the DSIM.

References

- [1] Ramirez A P 1994 *Annu. Rev. Mater. Sci.* **24** 453
- [2] Greedan J E 2001 *J. Mater. Chem.* **11** 37
- [3] Harris M J, Bramwell S T, McMorro D F, Zeiske T and Godfrey K W 1997 *Phys. Rev. Lett.* **79** 2554
- [4] Bramwell S T and Gingras M J P 2001 *Science* **294** 1495
- [5] Ramirez A P, Hayashi A, Cava R J, Siddharthan R and Shastry B S 1999 *Nature* **399** 333
- [6] Castelnovo C, Moessner R and Sondhi S L 2012 *Annu. Rev. Condens. Matter Phys.* **3** 35
- [7] Rosenkranz S, Ramirez A P, Hayashi A, Cava R J, Siddharthan R and Shastry B S 2000 *J. Appl. Phys.* **87** 5914
- [8] Jana Y M, Sengupta A and Ghosh D 2002 *J. Mag. Mag. Mater.* **248** 7
- [9] den Hertog B C and Gingras M J P 2000 *Phys. Rev. Lett.* **84** 3430
- [10] Zhou H D, Bramwell S T, Cheng J G, Wiebe C R, Li G, Balicas L, Bloxson J A, Silverstein H J, Zhou J S, Goodenough J B and Gardner J S 2011 *Nat. Commun.* **2** 478
- [11] Zhou H D, Cheng J G, Hallas A M, Wiebe C R, Li G, Balicas L, Zhou J S, Goodenough J B, Gardner J S and Choi E S 2012 *Phys. Rev. Lett.* **108** 207206
- [12] Cai Y Q, Cui Q, Li X, Dun Z L, Ma J, Dela Cruz C R, Jiao Y Y, Liao J, Sun P J, Li Y Q, Zhou J S, Goodenough J B, Zhou H D and Cheng J G 2016 *Phys. Rev. B* **93** 014443
- [13] Li X, Cai Y Q, Cui Q, Lin C J, Dun Z L, Matsubayashi K, Uwatoko Y, Sato Y, Kawae T, Lv S J, Jin C Q, Zhou J S, Goodenough J B, Zhou H D and Cheng J G 2016 *Phys. Rev. B* **94** 214429
- [14] Hoekstra H R and Gallagher F 1968 *Inorg. Chem.* **7** 2553
- [15] Tang Z, Li C Z, Yin D, Zhu B P, Wang L L, Wang J F, Xiong R, Wang Q Q and Shi J 2006 *Acta Phys. Sin.* **55** 6532 (in Chinese)
- [16] Fukazawa H, Melko R G, Higashinaka R, Maeno Y and Gingras M J P 2002 *Phys. Rev. B* **65** 054410
- [17] Matsuhira K, Hinatsu Y and Sakakibara T 2001 *J. Phys.: Condens. Matter* **13** L737
- [18] Snyder J, Ueland B G, Slusky J S, Karunadas H, Cava R J and Schiffer P 2004 *Phys. Rev. B* **69** 064414
- [19] Shi J, Tang Z, Zhu B P, Huang P, Ying D, Li C Z, Wang Y and Wen H 2007 *J. Mag. Mag. Mater.* **310** 1322
- [20] Snyder J, Ueland B G, Slusky J S, Karunadas H, Cava R J, Mizel A and Schiffer P 2003 *Phys. Rev. Lett.* **91** 107201